Strojniški vestnik - Journal of Mechanical Engineering 70(2024)9-10, 507-514
DOI:10.5545/sv-jme.2023.618
Original Scientific Paper
Received for review: 2023-04-24
Received revised form: 2023-09-19
Accepted for publication: 2023-09-25

Multi-Response Optimization of Single Point Incremental Forming of Al 6061 Sheet Through Grey-Based Response Surface Methodology

Thangavel Karthik[1,*] – Nagarajan Srinivasan[2] – Duraisamy Rajenthirakumar[1] – Ramasamy Sridhar[1]

[1] PSG College of Technology, Department of Mechanical Engineering, India
[2] Jansons Institute of Technology, Department of Mechanical Engineering, India

The single point incremental forming process (SPIF) is materialized to form the desired shapes in low-cost sheet metal processing and well suited for low batch components and customized designs. Many modifications have been attempted in recent years to maximize the formability, geometric accuracy and quality of the SPIF formed parts. In this work, an attempt has been made to analyse the influence of process parameters namely ball tool diameter, step size, spindle speed and sheet thickness on final wall thickness, forming force and surface roughness. The optimized results exhibit the desirable formability when the roller ball tool diameter of the tool is 12 mm. The results also project that formability of the sheet metal is minimized when the spindle speed is increased and the ball diameter maximizes the accuracy and surface roughness. Also minimizing the step size increases the product quality features. Upon conducting this multi-response optimization by grey based response surface methodology (RSM) technique It is identified that 12 mm ball diameter of the tool, 0.25 mm step size, 2445 rpm spindle speed, and 2 mm sheet thickness are the obtained optimized SPIF process parameters as confirmed through confirmation experiments.

Keywords: grey based RSM, single point incremental forming, roller ball tool, surface roughness

Highlights

- *Roller ball tool with different diameter is employed in SPIF process of Al 6061 sheets.*
- *Implementing a hybrid approach and a grey-based RSM technique, the process optimization is achieved.*
- *This study examines the correlation between the roller ball tool and the surface roughness of the resultant component over different ball tool diameters.*

0 INTRODUCTION

Single point incremental forming process (SPIF) is a manufacturing process which does not require a dedicated die for producing three dimensional (3D) manufacturing parts. SPIF is well-known for rapid prototyping and customized sheet metal components. SPIF process has better formability than conventional forming processes due to localized plastic deformations and through-thickness shearing deformations. This SPIF process employs a modest hemispherical tool to deform the sheet metal step by step (incrementally) by allowing in the generated tool path. A ball tool is utilized in incrementally forming sheet metal components. The ball rotates itself during the tool rotation in the prescribed tool path to achieve the deformed shape [1]. Tool diameter, step depth, feed rate, spindle speed, wall angle, and tool path are the influencing parameters that affects the mechanics of SPIF process [2]. High processing duration with less geometric accuracy than conventional process are the few significant restrictions in the SPIF process [3]. The response surface methodology (RSM) with neuro-fuzzy was developed to identify the response parameters based on the central composite design of experiments along with inverse analysis [4]. Honarpisheh et al. studied multi-response optimization to predict the process parameters and the authors validated through experiment reporting that 95 % of confidence interval between responses obtained and input parameters using RSM [5]. Chang et al. [6] developed an analytical model to predict the force related components in both axial and radial directions with maximum accuracy and reported that the deviations in force components are produced by varied elastic deflection of the sheet metal. Kumar and Gulati [7] optimized the process parameters of SPIF process and analysed the effect of forming force and thickness reduction of frustums using Taguchi method.

Sbayti et al. [8] experimented the optimization of geometric accuracy using hybrid grasshopper optimization algorithm and reported that changes in geometric shapes and defects with obtained geometry and geometry generated by computer aided design (CAD) can be obtained by simulations and optimization techniques. Taherkhani et al. [9] studied four process parameters using artificial neural network (ANN) and evaluated using genetic algorithm to obtain the prompt values for parameters. Ahiri et al. [10] optimized the SPIF process parameters in forming Al 5052 using ANN. The effect of ball nose tool upon

*Corr. Author's Address: Department of Mechanical Engineering, PSG College of Technology, India, tkarthik.psg@gmail.com

optimizing the process parameters results in expected quality in forming sheet metal parts.

In this study, a hybrid approach is used to combine Taguchi grey relational analysis (TGRA) and RSM in order to find the best possible set of input process parameters, including sheet thickness, roller ball tool diameter, spindle speed, and vertical step size, that will produce the best possible results.

1 DESIGN OF FORMING TRIALS AND EXPERIMENTATION

The SPIF sheet metal experiments were conducted using a five-axis MAKINO CNC vertical milling center (Fig. 1a). The aluminum 6061 sheet metal of dimensions 400 mm × 400 mm is employed in the fixture as shown in Fig. 1b.

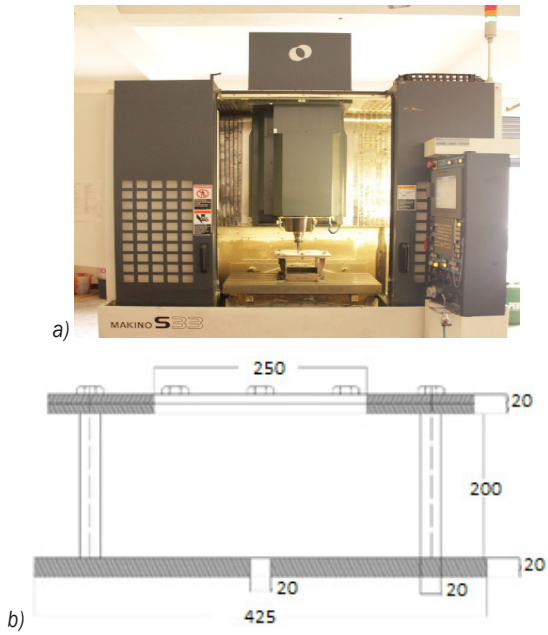

Fig. 1. a) *Three-axis CNC milling for incremental forming, and b) three dimensional fixture of SPIF process*

The aluminum 6061 has several applications in aerospace industries and possesses good formability towards the desired shape. The fixture consists of base plate, supporting plate and roller ball tool. The Al 6061 sheet metal blank is detained in the fixture with the backing of a supporting plate and a holding plate to eliminate the blank's movement during SPIF process. Since no specific lubricant has been adopted in this experiment, the usual water diluted lubricant is applied to minimize the excessive friction generated within the roller ball tool and Al 6061 blank material. The novel developed roller ball tool of HcHcr tool steel is considered in these experiments with diameters of 8 mm, 10 mm, and 12 mm which is vacuum hardened and achieve average hardness of 56 MPa as shown in Fig. 2.

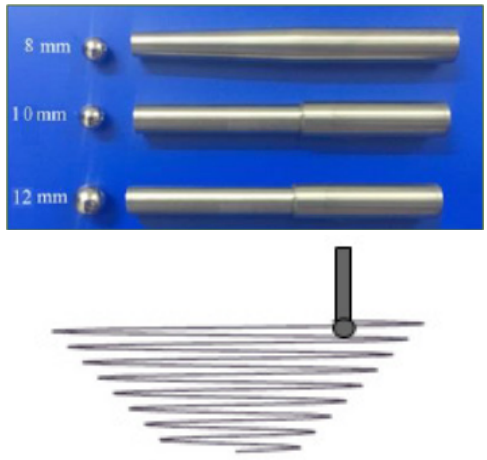

Fig. 2. *Roller ball tool and tool path rotation*

The significant attribute of the ball tool is its ability to generate minimum friction and achieve a high surface polish. This is attributed to its unrestricted rotational movement within its formed cavity.

SPIF process parameters are chosen which can produce a reasonable response value and impact on output parameters. The trials for experimentation are designed with Taguchi L27 orthogonal array (OA). It allows the parameter combination study among the other forming parameters. The trial count in L27 is less than the actual trial count essential in central composite design. The forming force, final wall thickness and surface roughness are measures of quality features in SPIF process of sheet metals and it are measured using a micrometer and Mitutoyo SJ-410 portable surface roughness tester respectively. The process parameters are varied at three significant levels responses on the impact on quality features are presented in Table 1.

2 GREY-BASED RESPONSE SURFACE METHODOLOGY (g-RSM)

Sheet metal forming components are expected to have a sufficient final wall thickness which can withstand the product functioning requirement and good aesthetics which can be produced by surface finish of the formed parts. This Taguchi method employs signal-to-noise (S/N) ratio to quantify the activity of the system **[11]**. The g-RSM uses the grey relational grade (GRG) to quantify. The multi-objective optimization

Table 1. *Responses obtained during experimental trials*

No. of experiment	Tool diameter [mm]	Step size [mm]	Sheet thickness [mm]	Spindle speed [rpm]	Forming force [N]	Final wall thickness [mm]	Surface roughness [μm]
1	8	0.25	1	1500	420.0	0.69	0.28
2	8	0.25	1.5	2000	780.0	1.46	0.32
3	8	0.25	2	2500	1080.0	1.62	0.35
4	8	0.5	1	2000	610.0	0.96	0.28
5	8	0.5	1.5	2500	730.0	0.97	0.32
6	8	0.5	2	1500	980.0	1.26	0.39
7	8	0.75	1	2500	460.0	1.45	0.36
8	8	0.75	1.5	1500	635.0	1.59	0.41
9	8	0.75	2	2000	760.0	1.46	0.38
10	10	0.25	1	1500	460.0	0.73	0.32
11	10	0.25	1.5	2000	620.0	1.50	0.34
12	10	0.25	2	2500	740.0	1.73	0.37
13	10	0.5	1	2000	720.0	0.99	0.31
14	10	0.5	1.5	2500	730.0	1.02	0.36
15	10	0.5	2	1500	980.0	1.31	0.43
16	10	0.75	1	2500	460.0	1.48	0.40
17	10	0.75	1.5	1500	635.0	1.63	0.45
18	10	0.75	2	2000	760.0	1.51	0.41
19	12	0.25	1	1500	483.7	0.80	0.36
20	12	0.25	1.5	2000	843.7	1.51	0.37
21	12	0.25	2	2500	1143.7	1.75	0.41
22	12	0.5	1	2000	673.7	1.03	0.34
23	12	0.5	1.5	2500	793.7	1.07	0.40
24	12	0.5	2	1500	1043.7	1.36	0.47
25	12	0.75	1	2500	523.7	1.55	0.44
26	12	0.75	1.5	1500	698.7	1.70	0.46
27	12	0.75	2	2000	823.7	1.55	0.48

problem reduced to optimization of a single response is achieved using the GRG calculation.

Step 1: Estimate the S/N ratio (η_{ij}) and carry out normalization as a portion of data pre-processing. Eqs. (1) and (2) were utilized to determine the S/N ratio and normalized S/N ratio (z_{ij}) **[12]**.

$$\text{S/N ratio} \quad \left(\eta_{ij}\right) = -10\log_{10}\left(\frac{1}{r}\sum_{i=1}^{n}\left(y_{ij}\right)^2 k\right), \quad (1)$$

$$Z_{ij} = \frac{y_{ij} - \min\left(y_{ij}, i = 1,2,\ldots,m\right)}{\max\left(y_{ij}, i = 1,2,\ldots,m\right) - \min\left(y_{ij}, i = 1,2,\ldots,m\right)}, \quad (2)$$

where r is the number of replication, n is the number of response, y_{ij} is the observed response value, m is the number of observation, $i = 1,2,..,m,\ k = 1,2,\ldots,r$ and $j = 1,2,..,m$.

Step 2: Compute the grey relational coefficient (GRC), γ_{ij} using Eq. (3) **[13]**.

$$\gamma_{ij} = \frac{\Delta\min + \xi\Delta\max}{\Delta_{oj}\left(i\right) + \xi\Delta\max}, \quad (3)$$

where ξ is the distinctive coefficient.

Step 3: Estimate the GRG by means of Eq. (4). The GRG converts multi into a single response **[13]**.

$$GRG_j = \frac{1}{n}\sum_{i=1}^{n}\gamma_{ij}. \quad (4)$$

Step 4: Construct a quadratic equation and perform analysis of variance (ANNOVA) on GRG values to study the impact of SPIF factors on the responses **[14]**.

Step 5: Create a 3D response graph to learn the effects of response parameters.

Step 6: Find the ideal combination of parameters and validate the response **[15]**.

4 RESULTS AND DISCUSSION

4.1 Computation of GRG Values

The data pre-processing is finished to keep the responses on a common scale, and the responses are normalized for additional analysis **[13]**. The S/N ratio, normalized S/N ratio and the GRCs are computed by means of the suitable equations defined above. The GRG values were suggestive of the system presentation **[9]**. The values of GRC and GRG are presented in Table 2. The GRG values are single representatives of multi-responses (forming force, final wall thickness and surface roughness) noticed during the forming trials. For better responses, a larger value of GRG is desirable. The ultimate value of GRG was found as 0.876 (trial number 21), exhibiting the optimal functioning condition. The GRG values for distinct trials are exhibited in Fig. 3. The disparities in the GRG values are by reason of the change in the process parameter deployed during trialling. The noteworthy discrepancies in GRG values for the different trials demonstrate the important effect of diverse levels of single point incremental process parameters.

Convergence in the plot specifies the smaller effect of parameter levels active during adjacent trials. Convergence in the plot indicates the minimum influence of parameter levels employed during adjacent testing. The absence of convergence in GRG values (Fig. 3) explicit the significant effect of process parameters levels preferred for this study.

4.2 Adequacy of Regression Model

The calculated GRG values are used as sole representatives of multiple responses. The identification of relationship among the SPIF process parameters are achieved by developing a mathematical model through RSM. Usage of L27 OA for conducting experiments authorize the study of contact amongst the SPIF process parameters with minimum experiments. A second order (quadratic model) polynomial equation is established with the aid of Design Expert software V12.0 that generates the coefficients of model using QR factorization method [16] and [17]. Eq. (5) represents the developed mathematical model.

$$\begin{aligned} GRG = {} & 0.630133 - 0.154830 \times Tool\,dia + 0.442984 \times Step\,size \\ & + 0.477371 \times Sheet\,thickness - 0.000089 \times Spindle\,speed \\ & + 0.020063 \times (Tool\,dia \times Sheet\,thickness) \\ & - 0.838938 \times (Step\,size \times Sheet\,thickness) \\ & + 0.007715 \times Tool\,dia^2 + 0.983983 \times Step\,size^2 \end{aligned} \quad (5)$$

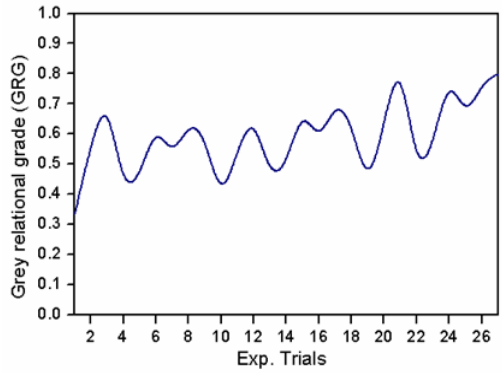

Fig. 3. *Variation of GRG for different experimental trials*

The model existing in Eq. (5) is devoid of insignificant relationships. ANOVA is performed in the GRG to explain the percentage contribution among the factors [16].

The model F value was detected to be 65.43 demonstrating its significance as shown in Table 3.

Table 2. *Normalization of responses and GRG values*

S/N Ratio			Normalized values			Grey relational coefficient			GRG grade	Rank
Forming force	Final wall thickness	Surface roughness	Forming force	Final wall thickness	Surface roughness	Forming force	Final wall thickness	Surface roughness		
–52.46499	–3.223018	11.056839	0.087	0.057	0.198	0.3333333	0.3333333	0.3333	0.3333333	27
–57.84189	3.2870571	9.8970004	0.618	0.805	0.248	0.5668587	0.7197618	0.3993	0.5619663	16
–60.66848	4.1903003	9.1186391	0.943	0.917	0.414	0.8973336	0.8577227	0.4604	0.7384869	5
–55.7066	–0.354575	11.056839	0.373	0.355	0.000	0.4434767	0.43662	0.3333	0.4044767	25
–57.26646	–0.264565	9.8970004	0.552	0.366	0.248	0.5273225	0.440907	0.3993	0.4558359	22
–59.82452	2.0074109	8.1787079	0.846	0.647	0.615	0.764294	0.5861855	0.5648	0.6384341	12
–53.25516	3.22736	8.87395	0.091	0.798	0.466	0.354814	0.7121908	0.4837	0.5168957	19
–56.05547	4.0279425	7.7443229	0.413	0.897	0.708	0.4598294	0.8291552	0.6310	0.63998	11
–57.61627	3.2870571	8.4043281	0.592	0.805	0.567	0.5506707	0.7197618	0.5357	0.6020313	14
–53.25516	–2.733543	9.8970004	0.091	0.061	0.248	0.354814	0.347355	0.3993	0.3671491	26
–55.84783	3.5218252	9.3704217	0.389	0.834	0.360	0.4499547	0.7511654	0.4387	0.5466001	18
–57.38463	4.7609221	8.6359655	0.565	0.988	0.517	0.5349855	0.9758944	0.5087	0.6731923	8
–57.14665	–0.087296	10.172766	0.538	0.388	0.189	0.5197746	0.4496011	0.3813	0.4502389	23
–57.26646	0.1720034	8.87395	0.552	0.420	0.466	0.5273225	0.4629542	0.4837	0.4913196	20
–59.82452	2.3454259	7.3306309	0.846	0.689	0.796	0.764294	0.6164025	0.7101	0.6969461	7
–53.25516	3.4052343	7.9588002	0.091	0.820	0.662	0.354814	0.7352344	0.5965	0.5621738	15
–56.05547	4.2437521	6.9357497	0.413	0.924	0.880	0.4598294	0.8675634	0.8068	0.711395	6
–57.61627	3.5795389	7.7443229	0.592	0.842	0.708	0.5506707	0.7593096	0.6310	0.6469786	9
–53.69152	–1.9382	8.87395	0.141	0.159	0.466	0.367907	0.3728388	0.4837	0.4081427	24
–58.52376	3.5795389	8.6359655	0.696	0.842	0.517	0.6221307	0.7593096	0.5087	0.6300458	13
–61.16624	4.860761	7.7443229	1.000	1.000	0.708	1	1	0.6310	0.8769852	1
–56.56933	0.2567445	9.3704217	0.472	0.430	0.360	0.4862374	0.4674917	0.4387	0.4641364	21
–57.99313	0.5876756	7.9588002	0.635	0.471	0.662	0.5782532	0.4860976	0.5965	0.5536079	17
–60.37151	2.6707782	6.5580428	0.909	0.729	0.961	0.8455445	0.6485835	0.9275	0.8072226	2
–54.38165	3.806634	7.1309465	0.220	0.870	0.839	0.3907088	0.7931469	0.7559	0.646597	10
–56.88581	4.6089784	6.7448434	0.508	0.969	0.921	0.5040668	0.9413596	0.8636	0.7696809	4
–58.31538	3.806634	6.3751753	0.672	0.870	1.000	0.604129	0.7931469	1.0000	0.7990919	3

Table 3. *ANOVA on GRG values*

Source	Sum of squares	DoF	Mean square	*F* value	*P* value Prob > *F*	
Model	0.5125	8	0.0641	65.43	< 0.0001	sign.
A-Tool diameter	0.0630	1	0.0630	64.29	< 0.0001	
B-Step size	0.0320	1	0.0320	32.64	< 0.0001	
C-Sheet Thickness	0.3008	1	0.3008	307.16	< 0.0001	
D-Spindle speed	0.0222	1	0.0222	22.72	0.0002	
AC	0.0048	1	0.0048	4.93	0.0394	
BC	0.0825	1	0.0825	84.23	< 0.0001	
A^2	0.0057	1	0.0057	5.84	0.0266	
B^2	0.0227	1	0.0227	23.18	0.0001	
Residual	0.0176	18	0.0010			
Cor Total	0.5302	26				

The effect of various SPIF process parameters and their relations is evidenced by the value of probability (p value < 0.05). The model fitness is revealed by the closeness of R-squared value (0.9668) to unity [16].

4.3 Study of Three-Dimensional Response Surfaces

The 3D surface response plots are generated to connect the GRG values with SPIF process parameters as shown in Fig. 4.

It is observed that the increase in sheet thickness necessitates an increase in tool diameter. It is evident that an increase in step size increases the irregularity in sheet thickness distribution irrespective of the sheet thickness. It is perceived from the plot that the step size and spindle speed show independence, because the increase in spindle speed and step size does not produce any additional force in stretching or material uniformity. Also, the increase in ball tool diameter doesn't generate significant effect on plastic deformation produced in the thinning effect on the sheet thickness. Considering the forming force, it increases with increase in ball tool diameter and sheet thickness.

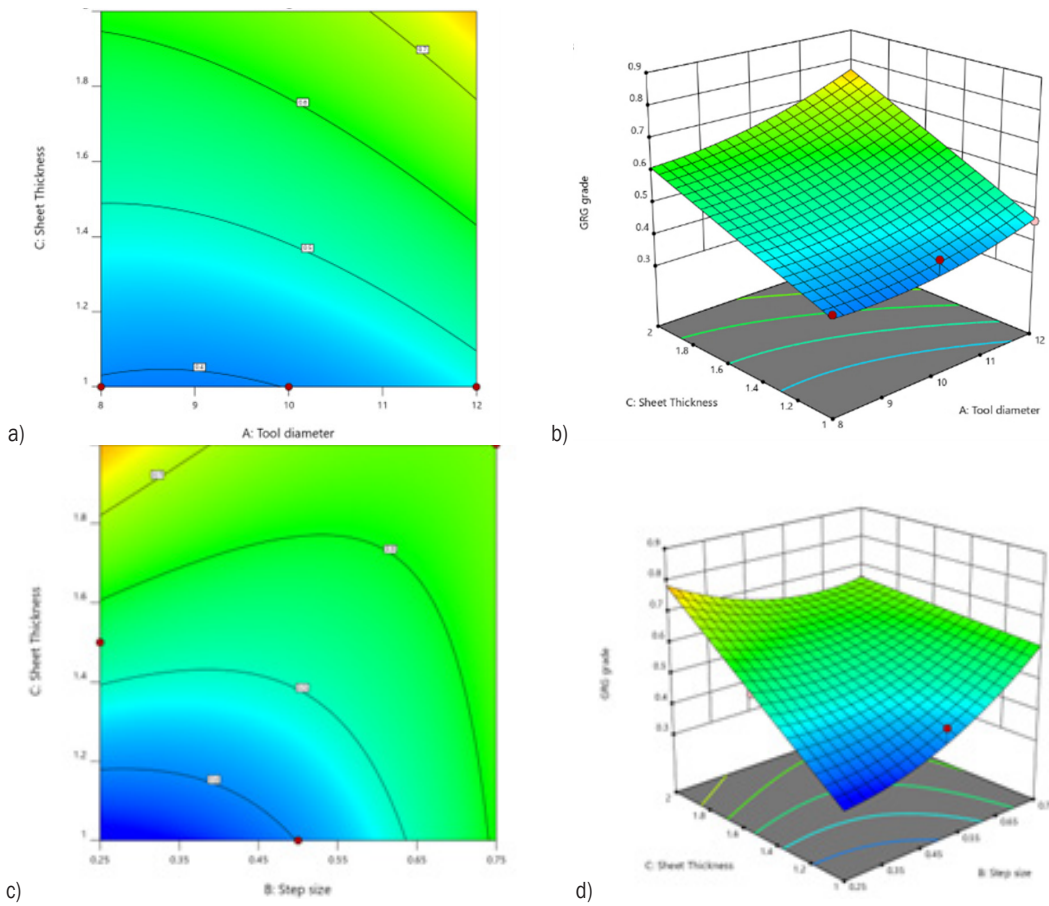

Fig. 4. *3D response surfaces and contour plots of input parameters; a) and c) GRG grade, s) and d) 3D surface*

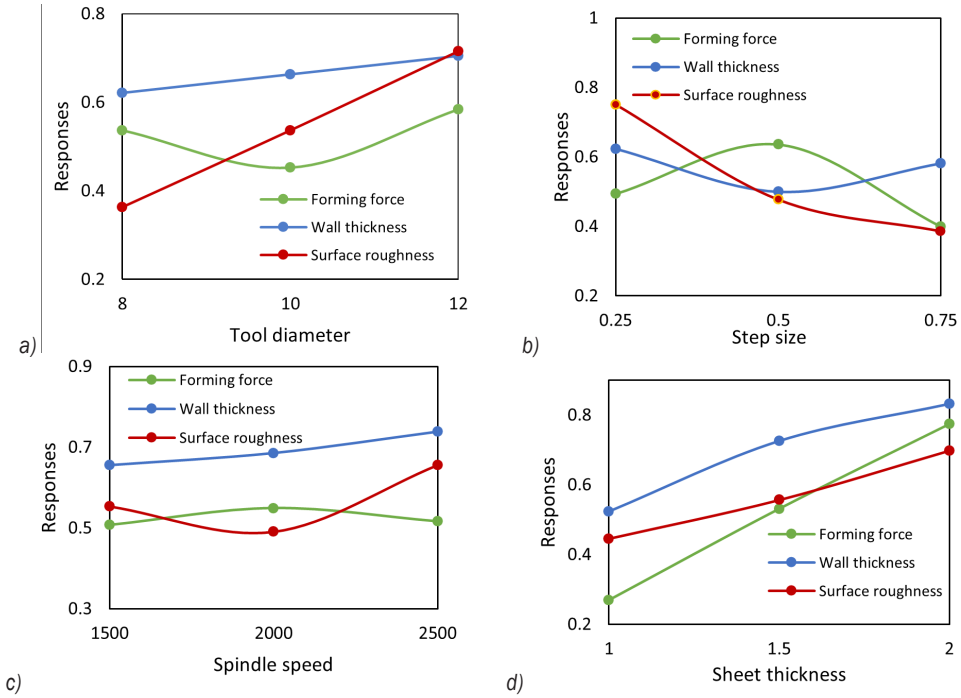

Fig. 5. *Effect of SPIF parameters on the responses*

4.4 Effect of SPIF Process Parameters on Responses

Fig. 5 shows the effect of SPIF process parameters on the response parameters. It is noted from the Fig. 5a that the increase in roller ball tool diameter increases the surface roughness of the formed sheet metal component. Also it supports uniform material distribution by maximizing the wall thickness [7]. The average surface roughness is achieved by plotting various spots of tool path. A decrease in step size encourages the increase in quality features like surface roughness and wall thickness as shown in Fig. 5b. Step size variation affects the surface roughness directly: minimum step size provides the maximum surface roughness and also the final wall thickness [18].

Considering the spindle speed in Fig. 5c, the plot displays that increase in spindle speed can produce good surface roughness and final wall thickness including minimum forming force. So, identifying the optimized spindle speed in SPIF process has a significant role in quality features of the components. From Fig. 5d, it exhibits that the increased sheet thickness produces good quality features and reduces the machine utilization like forming forces.

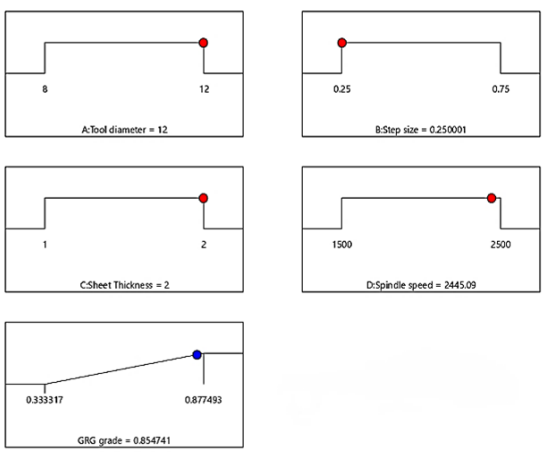

Fig. 6. *Desirability analysis*

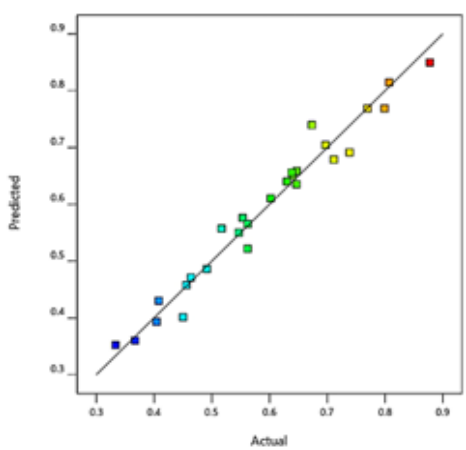

Fig. 7. *Plot of the predicted versus actual GRG values*

4.5 Desirability Analysis

The design Expert software is utilized to accomplish the desirability analysis [16]. The conclusions of desirability analysis are recorded.

Table 4 with optimal response parameters. The SPIF condition which exhibits the highest desirability value is opted as the ideal condition. The ideal condition of tool diameter is 12 mm, step size is 0.25001 mm, sheet thickness is 2 mm, spindle speed is 2445.2 r/min and GRG grade is 0.854741 is shown in Fig 6. The predicted vs. actual graph (Fig. 7) shows the unvarying form which are close to a straight line, ensures the correctness of the predicted values.

Table 4. *Confirmation test*

Parameter setting	GRG	Responses		
		Forming force	Final wall thickness	Surface roughness
Optimal setting	0.33333	420.0	0.69	0.28
Optimal setting using g-RSM	0.876985	1143.7	1.75	0.41
Improvement	0.543655	723.7	1.06	0.13
Improvement [%]	61.99	63.28	60.57	31.71

4.6 Experiments of Confirmations

The optimized parameters are experimented to validate and approve the g-RSM approach. The responses attained with the initial settings of SPIF parameters are compared with those obtained with the optimal operating condition predicted by g-RSM method. It is noted that good agreement between confirmation experiments, GRG optimized values and the formed components are found to be accurate as shown in Fig. 8. The scanning electron microscope (SEM) fractography outputs are presented in Fig. 8 which infers that the sheets developed under an evolution from shear to inter-crystalline separation with a considerable amount of plastic deformation along with inter-crystalline fracture. Based upon the optimization technique and SEM results, it can be determined that forming two sheet blanks in SPIF process would be idyllic.

5 CONCLUSIONS

The process parameters of SPIF have been optimized using grey based response surface methodology and the optimized parameters have been identified. The effect on optimized parameters is studied on response parameters. The experiments of confirmation are conducted to validate the optimized parameters. Based on this, the following conclusions are made:

1. Increase in roller ball tool diameter increases the surface roughness of the formed part and increases the uniformity in sheet metal

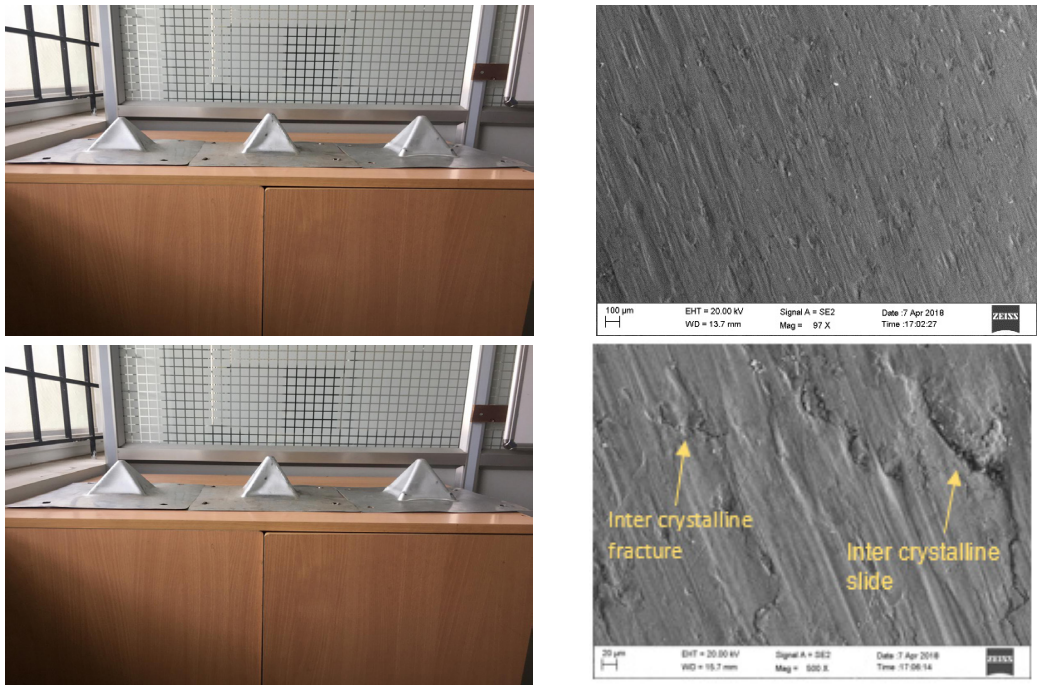

Fig. 8. *Confirmation test results and its fractography*

distribution. 12 mm ball tool is identified as the optimum tool diameter for 2 mm sheet thickness.

2. Reducing the step size increases the material formability and quality features and supports thickness distribution. It is found that 0.25 mm step size is an optimal value for the present process condition.
3. Increase in spindle speed promotes the augmentation of surface roughness and final wall thickness while simultaneously limiting the exertion of forming force which is identified as 2445.5 r/min.
4. It is evident that the increased sheet thickness produces good quality features with an increase in the forming force. From this study it is identified that the optimal sheet thickness is 2 mm.

The practice of the single point incremental forming technology can greatly assist in the fabrication of non-identical indigenous components.

8 REFERENCES

[1] Karthik T., Rajenthirakumar D., Srinivasan N., Sridhar R. (2019) Influence of roller ball tool in single point incremental forming of polymers. *Technical Gazette*, vol. 26, no. 1, p. 171-176, **DOI:10.17559/TV-20180809113703**.

[2] Martins, P.A.F., Bay, N., Skjoedt, M., Silva, M.B. (2008) Theory of single point incremental forming. CIRP Annals, vol. 57, no. 1, p. 247-252, **DOI:10.1016/j.cirp.2008.03.047**.

[3] Jeswiet, J., Micari, F., Hirt, G., Bramley, A., Duflouu, J., Allwood, J. (2005). Asymmetric single point incremental forming of sheet metal. *CIRP Annals*, vol. 54, no. 2, p. 88-114, **DOI:10.1016/S0007-8506(07)60021-3**.

[4] Maji, K., Kumar, G. (2020). Inverse analysis and multi-objective optimization of single-point incremental forming of AA5083 aluminum alloy sheet. *Soft Computing*, vol. 24, p. 4505-4521, **DOI:10.1007/s00500-019-04211-z**.

[5] Honarpisheh, M., Mohammadi Jobedar, M., Alinaghian, I. (2018) Multi-response optimization on single-point incremental forming of hyperbolic shape Al-1050/Cu bimetal using response surface methodology. *International Journal of Advanced Manufacturing Technology*, vol. 96, p. 3069-3080, **DOI:10.1007/s00170-018-1812-5**.

[6] Chang, Z., Li, M., Chen, J. (2019) Analytical modeling and experimental validation of the forming force in several typical incremental sheet forming processes. *International Journal of Machine Tools and Manufacture*, vol. 140, p. 62-76, **DOI:10.1016/j.ijmachtools.2019.03.003**.

[7] Kumar, A., Gulati, V. (2020). Optimization and investigation of process parameters in single point incremental forming. *Indian Journal of Engineering and Material Sciences*, vol. 27, no. 2, p. 246-255, **DOI:10.56042/ijems.v27i2.45925**.

[8] Sbayti, M., Bahloul, R., Belhadjsalah, H. (2020). Efficiency of optimization algorithms on the adjustment of process parameters for geometric accuracy enhancement of denture plate in single point incremental sheet forming. *Neural Computing and Applications*, vol. 32, p. 8829-8846, **DOI:10.1007/s00521-019-04354-y**.

[9] Taherkhani, A., Basti, A., Nariman-Zadeh, N., Jamali, A. (2019) Achieving maximum dimensional accuracy and surface quality at the shortest possible time in single-point incremental forming via multi-objective optimization. *Proceedings of the Institution of Mechanical Engineers, Part B: Journal of Engineering Manufacture*, vol. 233, no. 3, p. 900-913, **DOI:10.1177/0954405418755822**.

[10] Azhiri, R.B., Rahimidehgolan, F., Javidpour, F., Tekiyeh, R.M., Moussavifard, S.M., Bideskan, A.S. (2020). Optimization of single point incremental forming process using ball nose tool. *Experimental Techniques*, vol. 44, p. 75-84, **DOI:10.1007/s40799-019-00338-8**.

[11] Gulati, V., Aryal, A., Katyal, P., Goswami, A. (2016). Process parameters optimization in single point incremental forming. *Journal of The Institution of Engineers (India): Series C*, vol. 97, p. 185-193, **DOI:10.1007/s40032-015-0203-z**.

[12] Baruah, A., Pandivelan, C., Jeevanantham, A.K. (2017). Optimization of AA5052 in incremental sheet forming using grey relational analysis. *Measurement*, vol. 106, p. 95-100, **DOI:10.1016/j.measurement.2017.04.029**.

[13] Raju, C., Sathiya Narayanan, C. (2016). Application of a hybrid optimization technique in a multiple sheet single point incremental forming process. *Measurement*, vol. 78, p. 296-308, **DOI:10.1016/j.measurement.2015.10.025**.

[14] Asghari, S.A.A., Shamsi Sarband, A., Habibnia, M. (2017). Optimization of multiple quality characteristics in two-point incremental forming of aluminum 1050 by grey relational analysis. *Proceedings of the Institution of Mechanical Engineers, Part C: Journal of Mechanical Engineering Science*, vol. 0, no. 0, **DOI:10.1177/0954406217693658**.

[15] Najm, S.M., & Paniti, I. (2021). Artificial neural network for modeling and investigating the effects of forming tool characteristics on the accuracy and formability of thin aluminum alloy blanks when using SPIF. *The International Journal of Advanced Manufacturing Technology*, vol. 114, p. 2591-2615, **DOI:10.1007/s00170-021-06712-4**.

[16] Liu, F., Li, Y., Yuan, H., Sun, R., Li, F., Li, J. (2022). Comprehensive modeling of forming forces in three directions for incremental sheet forming process based on the contact area. *Journal of Manufacturing Processes*, vol. 84, p. 986-1000, **DOI:10.1016/j.jmapro.2022.10.066**.

[17] Santhanakumar, M., Adalarasan, R., Rajmohan, M. (2015). Experimental modelling and analysis in abrasive waterjet cutting of ceramic tiles using grey-based response surface methodology. *Arabian Journal for Science and Engineering*, vol. 40, p. 3299-3311, **DOI:10.1007/a13369-015-1775-x**.

[18] Trzepieciński, T., Kubit, A., Dzierwa, A., Krasowski, B., Jurczak, W. (2021). Surface finish analysis in single point incremental sheet forming of rib-stiffened 2024-T3 and 7075-T6 alclad aluminium alloy panels. *Materials*, vol. 14, no. 7, art. ID 1640, **DOI:10.3390/ma14071640**.